Journal of Chromatography, 332 (1985) 71–106
Elsevier Science Publishers B.V., Amsterdam — Printed in The Netherlands

CHROMSYMP. 612

SEPARATION OF FREE RADICALS BY HIGH-PERFORMANCE LIQUID CHROMATOGRAPHY WITH ELECTRON SPIN RESONANCE DETECTION

KEISUKE MAKINO*,*, FUMIO MORIYA** and HIROYUKI HATANO
Department of Chemistry, Faculty of Science, Kyoto University, Kitashirakawa, Sakyo-ku, Kyoto 606 (Japan)
(Received March 29th, 1985)

SUMMARY

Studies on the separation of free radicals by high-performance liquid chromatography with electron spin resonance detection (HPLC–ESR) are described. Aqueous solutions of amino acids, dipeptides and tripeptides were γ-irradiated in the presence of a spin trap, 2-methyl-2-nitrosopropane. The stable aminoxyl radicals (spin adducts) produced were isolated by HPLC on cation-exchange columns. An ESR spectrometer was utilized as a detector for monitoring the eluted radicals. Various types of spin adducts were identified and characterized by ESR spectroscopy. The individual components of several pairs of diastereomeric radicals could be separated.

INTRODUCTION

Free radicals are considered to be important intermediates of reactions occurring in living tissues[1]. The detection of radical species generated from biologically important molecules by high energy, *e.g.*, ionizing radiation, is very important in exploring the mechanisms of the induced reactions in biological systems[2,3]. However, especially in aqueous solutions, ambiguous assignments have been made, mainly because of the short life of the species.

In order to overcome this problem, the method of spin trapping was developed by several research groups[4–11] and subsequently applied in biochemistry[12,13]. In this method, short-lived free radicals are converted into relatively stable aminoxyl radicals (spin adducts) through reactions with spin traps such as nitroso or nitrone compounds. The lifetimes of spin adducts are often of the order of minutes or hours. Therefore, one can carry out electron spin resonance (ESR) measurements of the spin adducts, and by analyzing the resulting spectra, can determine the structures of the original short-lived radicals.

* Present address: Department of Polymer Science and Engineering, Faculty of Textile Science, Kyoto Institute of Technology, Matsugasaki, Sakyo-ku, Kyoto 606, Japan.
** Present address: Department of Chemistry, Kobe University of Commerce, Tarumi-ku, Kobe 655, Japan.

0021-9673/85/$03.30

The spin-trapping method can be applied to reactions of aqueous systems by use of water-soluble spin traps and, therefore, has been extensively utilized to study short-lived free radicals produced in aqueous solutions of biomolecules by ionizing radiations, photochemical reactions, etc.[14–27]. In this way, many short-lived radicals not previously detected by conventional methods were identified. However, as the number of applications increased, a problem arose. As expected, in many systems, several different types of short-lived radicals are produced and can be spin-trapped simultaneously. In such cases, it is not easy to identify each of the components because of the overlap of several different ESR spectra due to the similarity in g values of the spin adducts. Liquid chromatography has been employed together with ESR spectroscopy for the separation and detection of radical mixtures[28]. This technique has been applied to the spin adducts in γ-irradiated aqueous solutions of several nucleotides[29,30] using 2-methyl-2-nitrosopropane (MNP) as a spin trap.

In the present work, we developed this technique further by employing high-performance liquid chromatography (HPLC). Our technique, called spin-trap HPLC–ESR, was applied to γ-irradiated aqueous solutions of amino acids, dipeptides and tripeptides containing MNP. The reaction of MNP with short-lived free radicals (·R) is represented by:

$$tert.\text{-Bu-N}=\text{O} + \cdot\text{R} \rightarrow tert.\text{-Bu–N(O}\cdot\text{)–R} \leftrightarrow tert.\text{-Bu–}\dot{\text{N}}^{+}(\text{O}^{-})\text{–R} \qquad (1)$$

It is well known that γ-radiolysis of water gives rise to highly reactive species such as hydroxyl radicals (·OH), hydrated electrons (e_{aq}^{-}) and hydrogen atoms (·H)[31,32]. Spin adducts produced by the reaction of such active species with the amino acids and peptides were separated and detected. Various types of spin adducts were identified and characterized by ESR spectroscopy. Several pairs of diastereomeric radicals having mutually different hyperfine splitting constants (h.f.s.c.s) were separated.

EXPERIMENTAL

MNP was synthesized as described previously[33]. Immediately prior to use, aqueous MNP solutions (*ca.* 57 m*M*) were prepared with stirring at 45°C for 1 h in the dark. The samples, amino acids (0.06–1.0 *M*) and di- and tripeptides (0.1 *M*), were dissolved in the MNP solutions. The resulting solutions were irradiated in a ^{60}Co γ-cell at dose rates of 4.5–6 kGy/h and a total dose of 3 kGy (unless otherwise specified) at ice temperature. The sample solutions were not deaerated because dissolved MNP is easily lost.

Immediately after irradiation, the sample solutions (1–1.7 ml) were separated by HPLC–ESR, the flow diagram for which is shown in Fig. 1. The columns contained cation exchangers (IEX-210SC, 60 × 0.75 cm unless otherwise specified) from Toyo Soda Manufacturing Co., Tokyo. The high-performance liquid chromatograph was a Toyo Soda Model HLC-803. All the separations were performed in the dark. The ESR spectrometer (JEOL, Model PE-3X, X-band, 100-kHz field modulation) used as a detector was set up as illustrated in Fig. 1. An UV flow monitor (Schoeffel Flow Monitor SF-770 or JASCO UVIDEC 100) was tuned to 240 nm. A quartz flow cell (working part 5 cm × 0.6 mm I.D.) was placed in the cavity of the ESR detector and connected to the column exit with PTFE tubing (0.25 mm I.D.). The exit of the

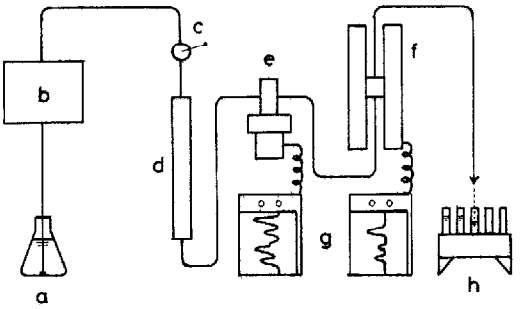

Fig. 1. Flow diagram of HPLC–ESR system. a = Eluents; b = pump; c = sample injector; d = column; e = UV detector; f = ESR detector; g = recorders; h = fraction tubes.

cell was connected to the UV monitor. In order to detect radicals passing through the ESR cavity during chromatography, the magnetic field was fixed at the position where the ESR signals were expected. For example, the fixed positions are indicated by the vertical arrows in Figs. 2, 6a, 8a–d and 12a. The amplitude of the magnetic field modulation applied was 1 mT unless specified otherwise.

The eluents used for the chromatographic separations of the spin adducts were Na_2HPO_4–NaH_2PO_4, NaOH–H_3BO_3 · NaCl and/or NaOH–Na_2HPO_4 buffers. In order to improve the retention, in some experiments, stepwise or gradient elution was applied. Other chromatographic conditions were as follows: pressure, 10–100 kg/cm^2; flow-rate, 0.1–0.3 ml/min; temperature, *ca.* 25°C.

The spin adducts isolated in the chromatographic fractions were identified by conventional ESR measurements carried out at *ca.* 25°C in the dark. Before the measurements, a gentle stream of nitrogen was passed through some of the fractions for *ca.* 1 min to remove dissolved oxygen which broadens the ESR spectral lines. The h.f.s.c.s were measured by using Mn^{2+} in MgO as a reference. To obtain accurate h.f.s.c.s, simulation of the ESR spectra was carried out by using a JEOL JEC-980A microcomputer. The line shapes adopted for the simulation were Lorentzian. The UV-VIS absorption spectra were recorded with a Cary 17 spectrophotometer (Varian, Palo Alto, CA, U.S.A.). Ninhydrin-positive fractions were analyzed by an amino acid analyzer (KLA-3B; Hitachi, Japan).

RESULTS AND DISCUSSION

Preparation of aqueous MNP solutions[34,35]

MNP is not very stable in aqueous solution. In the present investigation, the aqueous MNP solutions should not contain contaminants which may prevent adequate spin trapping, form free radicals and produce spin adducts interfering with accurate ESR analysis. Therefore, detailed studies were made of the aqueous MNP solutions.

MNP is known to exist as a dimer in the solid state and to participate in a monomer–dimer equilibrium in solution[33]:

$$\underset{\text{(monomer)}}{2\ \textit{tert.}\text{-Bu–N=O}} \rightleftarrows \underset{\text{(dimer)}}{\textit{tert.}\text{-Bu–N}^{+}(\text{O}^{-})=\text{N}^{+}(\text{O}^{-})\text{–}\textit{tert.}\text{-Bu}} \qquad (2)$$

The forward and backward reactions in aqueous solutions are slow compared to those in other solvents. For example, it takes 12 h at 30°C in aqueous solution to obtain the maximum concentration of the monomer. Since short-lived free radicals can be spin-trapped only by the monomer a sufficient concentration of the monomer is required. The concentrations of monomer and dimer in aqueous solution are determined by observing the absorbance at 662 nm (molar extinction coefficient, $\varepsilon \approx 20$ l mol^{-1} cm^{-1})[36] and 287 nm ($\varepsilon \approx 8000$ l mol^{-1} cm^{-1})[36].

Upon incubating aqueous MNP solutions at 45°C, an absorption band other than those due to the two forms of MNP was observed at 224 nm and grew with time. The relevant compound could be separated by HPLC on the cation exchanger and identified as *tert.*-butylnitrosohydroxylamine which is produced by heterolytic cleavage of the MNP dimer:

$$\textit{tert.}\text{-Bu–N}^{+}(\text{O}^{-})=\text{N}^{+}(\text{O}^{-})\text{–Bu-}\textit{tert.} \rightarrow \textit{tert.}\text{-Bu–N}^{+}(\text{O}^{-})=\text{N–O}^{-} + \underset{\text{CH}_3\text{–C}^{+}(\text{CH}_3)_2}{}$$

$$\xrightarrow{\text{H}_2\text{O}} \textit{tert.}\text{-Bu–N(OH)–N=O} + \textit{tert.}\text{-BuOH} + \text{CH}_2=\text{C(CH}_3)_2 \qquad (3)$$

The concomitant formation of *tert.*-butyl alcohol and isobutene was also confirmed by gas chromatography and NMR spectroscopy.

Since γ-radiolysis of the sample solutions in the presence of these undesirable contaminants leads to complex ESR spectra which are extremely difficult to analyze, the aqueous MNP solutions were prepared by stirring an aqueous suspension of the dimer for less than 2 h at 45°C and used immediately afterwards.

Separation of spin adducts from MNP[37,38]

In order to develop the method of HPLC separation and ESR analysis for spin adducts from biologically important molecules, the fundamental separation conditions had to be determined. When aqueous solutions, for instance, of amino acids were γ-irradiated in the presence of MNP, spin adducts were formed from the spin trap as well as from the solutes. As a preliminary, therefore, the separation of the spin adducts generated from MNP by γ-radiolysis was performed using an IEX-210SC column (60 × 0.4 cm).

When an aqueous MNP solution prepared by stirring for more than 2 h was irradiated, the ESR spectrum shown in Fig. 2 was produced. Upon loading the same sample on the column and using borax–sodium hydroxide buffer (*ca.* 60 m*M*, pH 11.5) as an eluent, five peaks (A–E) due to the MNP spin adducts appeared in the chromatogram as shown in Fig. 3. The production of negative or positive peaks was dependent both on the constant magnetic field and on the ESR signals detected in the derivative mode. Peak A, eluted near the void volume, produced an ESR spectrum comprised of 3 × 3 lines due to the aminoxyl nitrogen and two equivalent β-hydrogens. The h.f.s.c.s obtained are listed in Table I. When the pH of the solution was varied from 11.5 to 4.5, a reversible spectral change was observed. At pH 6.0, the spectrum observed corresponded to a superimposition of those at pH 11.5 and 4.5, with equal intensities. Consequently the pK_a value of the adduct could be determined to be 6.0, which corresponds to the value of *tert.*-butylnitrosohydroxylamine[34,35]. The first peak was also found to increase as a function of the time required to prepare

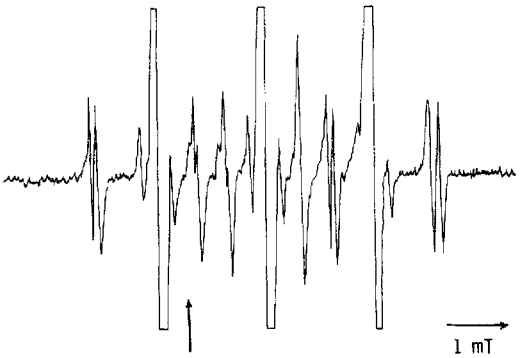

Fig. 2. ESR spectrum of a γ-irradiated aqueous MNP solution adjusted to pH 12.0 after irradiation. During chromatography, the magnetic field of the ESR detector was fixed at the position indicated by the vertical arrow.

the aqueous MNP solutions. The spectrum was assigned to the adduct from *tert.*-butylnitrosohydroxylamine:

$$\textit{tert.}\text{-Bu–N(O}^{\bullet}\text{)–CH}_2\text{–C(CH}_3\text{)}_2\text{–N(OH)–N=O (at pH 4.5)} \qquad \text{I}$$

Since spin adduct I has a retention time similar to those of the adducts from the substrates studied, the proposed procedure for preparing aqueous MNP solutions is useful in reducing the generation of adduct I, which interferes with the analysis of the ESR spectra obtained. The other four spin adducts from MNP were eluted slowly, whereas the spin adducts from the amino acids and peptides investigated were eluted much more rapidly, without separation. In this work, therefore, eluents weaker than the buffer used for the MNP adducts were utilized for the separation of adducts from the amino acids and peptides. This led to significantly increased elution volumes of the MNP adducts.

Peak B gave rise to 3 × 4 lines in the ESR spectrum, due to the aminoxyl nitrogen and three equivalent β-hydrogens. The h.f.s.c.s are shown in Table I. This spectrum was assigned to the spin adduct of the methyl radical, *tert.*-Bu–N(O•)–CH_3 (II). The parent radical was produced by the C–C bond scission in MNP upon γ-radiolysis.

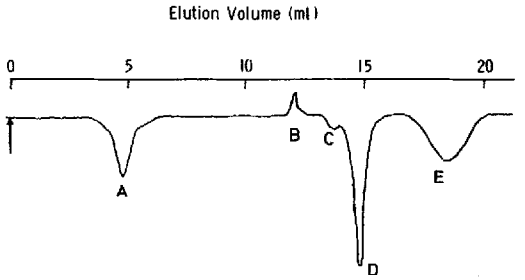

Fig. 3. Chromatogram of a γ-irradiated aqueous MNP solution. The ordinate is relative signal intensity obtained by ESR detection. The eluent was a borax–sodium hydroxide buffer (*ca.* 60 m*M*, pH 11.5).

TABLE I

H.F.S.C.S OF THE SPIN ADDUCTS FROM MNP

Spin adduct	*pH*	*h.f.s.c. (mT)*	
		a_N	$a_{\beta H}$
I	11.5	1.62	1.01 (2H)
	4.5	1.62	1.14 (2H)
II	11.5	1.73	1.42 (3H)
III	11.5	1.66	1.11 (2H)
Unidentified	11.5	1.68	
IV	11.5	1.72	

Peak C gave an ESR spectrum consisting of 3 × 3 lines attributed to the aminoxyl nitrogen and two equivalent β-hydrogens. The h.f.s.c.s obtained are shown in Table I and were found to be pH-independent. The structure tentatively assigned to the adduct is:

tert.-Bu–N(O•)–$CH_2C(CH_3)_2N=O$ (monomeric)

or III

tert.-Bu–N(O•)–$CH_2C(CH_3)_2N^+(O^-)=N^+(O^-)$–*tert.*-Bu (dimeric)

The ESR spectra of peaks D and E were simple triplets having different N-h.f.s.c.s. The value for peak D was 1.68 mT and that for E was 1.72 mT. The spin adduct of peak E was identified as di-*tert.*-butylnitroxide (DTBN), *tert.*-Bu–N(O•)–Bu-*tert.* (IV). The 1.68-mT triplet has not been identified, although the height of peak D was found to correspond to the concentration of the MNP dimer in the solution before irradiation.

Post radiolysis growth of ESR spectra[35]

It has been previously reported that the ESR signals of the spin adducts produced in aqueous thymine solutions light-irradiated in the presence of MNP was increased in intensity during storage[21,27]. A similar behaviour has been found for some aminoxyl radicals[39–41]. In the present work, the increase in the signal due to DTBN produced upon γ-irradiation of aqueous MNP solutions (initial pH 4–5) with increasing pH was observed. Spectrophotometric evidence was found for the formation of nitrous acid and it was shown that some of the spin adducts produced in the solution formed diamagnetic species and were then converted gradually into their paramagnetic form by hydrolysis. The mechanism proposed is as follows: monomeric MNP is cleaved into free radicals, •NO and *tert.*-Bu•, upon irradiation:

$$tert.\text{-Bu–N=O} \rightarrow \text{•NO} + tert.\text{-Bu•} \quad (4)$$

Nitrous acid is produced from •NO

$$\text{•NO} + 1/2\ O_2 \rightarrow NO_2 \quad (5)$$

$$\text{•NO} + NO_2 + H_2O \rightleftarrows 2\,HNO_2 \quad (6)$$

and then partially oxidized to nitric acid

$$HNO_2 \rightarrow HNO_3 \tag{7}$$

resulting in a lowering of the pH. The produced *tert.*-butyl radical is spin-trapped by MNP:

$$tert.\text{-}Bu^{\cdot} + tert.\text{-}Bu\text{–}N=O \rightarrow tert.\text{-}Bu\text{–}N(O^{\cdot})\text{–}tert.\text{-}Bu \tag{8}$$

Spin adducts as well as DTBN form diamagnetic intermediates (Y^{n+}) at low pH through the reaction with nitrous acid

$$\text{Spin adduct} + HNO_2 + X \xrightarrow{H^+} Y^{n+} \tag{9}$$

where X is a diamagnetic compound which could not be identified in this work. By raising the pH, the intermediates (Y^{n+}) are decomposed releasing the original spin adducts[42]:

$$Y^{n+} \xrightarrow{OH^-} \text{Spin adduct} + \cdot NO + NO_2 + X \tag{10}$$

As explained above, the increase in the signal intensity during storage is not due to the generation of new radicals but due to the release of the adducts.

Columns for separation of spin adducts from amino acids and peptides

Although aminoxyl radicals are relatively stable in solution, they are still readily decomposed on the columns. In this work, therefore, column selection was made carefully so that all the spin adducts produced from the amino acids and peptides could be detected.

Silica-based columns are used most extensively for the purification and identification of biological samples. In the separation of the spin adducts, however, such columns were found to inactivate the radicals. Only polymer-based ion-exchange columns yielded acceptable results. The eluents used for the ion exchangers were unique. Usually, with a cation exchanger, slightly acidic solutions are employed to keep the samples cationic. On the contrary, we found that neutral or basic buffers yielded better separations of the spin adducts from the amino acids and peptides studied. Also, many of the radicals were better isolated on cation exchangers than on anion-exchange columns. Consequently, the separation of the adducts was exclusively carried out by use of a cation-exchange column, IEX-210SC (Toyo Soda), containing sulphonated styrene–divinylbenzene copolymer. First, it was determined whether radicals were generated during the chromatography. Aqueous solutions containing amino acids and MNP without γ-irradiation were loaded on the column and no ESR signals were detected from the eluates. In another experiment, samples were injected which had been prepared by adding aqueous MNP solutions to γ-irradiated solutions containing only amino acids. No spin adducts were detected in the eluates. Consequently IEX-210SC columns were employed throughout this work.

Separation of spin adducts from amino acids

Free radicals generated from twelve amino acids by γ-irradiation of their aqueous solutions were investigated by spin-trap HPLC–ESR. In a preliminary experiment using the IEX-210SC column (60 × 0.75 cm unless specified otherwise), it was found that negatively charged spin adducts were eluted much more rapidly than neutral, positively charged or zwitterionic spin adducts in neutral or basic eluents. Most spin adducts produced by the self-trapping of MNP[37,38] were adsorbed on the column and were eluted very slowly with diffusion. The ESR signal intensities of these broad chromatographic peaks were so small that they were not always observable.

Glycine[43]. An aqueous solution of glycine (1.0 *M*) containing MNP was loaded on the column immediately after irradiation and subsequent addition of 2 *M* sodium phosphate buffer. A 0.2 *M* sodium phosphate buffer, pH 7.0, was used as an eluent. In the chromatogram obtained by ESR detection, three peaks appeared. Since it is well known that irradiation of water results in generation of highly reactive primary species, mainly hydrated electrons (e_{aq}^-), hydroxyl radicals (·OH) and hydrogen atoms (·H)[31,32], the reactions involving these species were considered to be responsible for the formation of the spin adducts giving rise to the peaks.

The first peak appeared close to the void volume and the fraction corresponding to it yielded an ESR spectrum comprised of a triplet arising from the aminoxyl nitrogen each line of which was further split into a 1:2:1 triplet. Since the latter triplet is due to two equivalent hydrogens, the spin adduct was identified as

tert.-Bu–N(O·)–CH_2–COO^- V

which was produced by the deamination reaction caused by the attack of e_{aq}^- and subsequent spin trapping. The reaction of e_{aq}^- with amino acids leads to reductive deamination[44,45]:

$$NH_3^+–CH(R)–COO^- + e_{aq}^- \rightarrow$$
$$NH_3^+–CH(R)–{\cdot}C(O^-)–O^- \rightarrow NH_3 + {\cdot}CH(R)COO^- \quad (11)$$

This assignment is supported by the rapid elution of the peaks. The h.f.s.c.s obtained are listed in Table II. In neutral and alkaline solutions, the spectral pattern of adduct V was pH-independent, which implies the absence of an amino group. However, in the pH range *ca.* 2–4, reversible pH-dependent shifts of the signals were observed, and could be attributed to the acid dissociation of the carboxyl group whose pK_a value is *ca.* 3.

The second peak exhibited an ESR spectrum interpreted as a triplet further split into five lines with the intensity ratio of 1:1:2:1:1 upon raising the pH to 11.1 at which the adduct was relatively stable. The 1:1:2:1:1 splitting pattern was due to a β-hydrogen and a β-nitrogen. The h.f.s.c.s obtained by the computer simulation are shown in Table II. The spin adduct was assigned to structure VI:

tert.-Bu–N(O·)–$CH(NH_2)COO^-$ VI

This adduct is derived from a short-lived radical produced by hydrogen abstraction

TABLE II

H.F.S.C.S OF THE SPIN ADDUCTS FROM GLYCINE, L-ALANINE, AND L-VALINE

Spin adduct	*pH*	*h.f.s.c. (mT)*			
		a_N	$a_{\beta H}$	$a_{\beta N}$	$a_{\gamma H}$
Glycine					
V	7.0	1.61	0.845 (2H)		
	1.4	1.58	0.86 (2H)		
VI	11.1	1.59	0.33	0.15	
L-Alanine					
VII	7.0	1.61	0.53		0.042 (3H)
	1.3	1.59	0.27		0.035 (3H)
VIII	7.0	1.64	1.67		0.045
			1.09		
	7.0 (80°C)	1.65	1.54		
			1.13		
	10.5	1.66	1.41		0.065
			1.09		
	1.7	1.63	1.63		0.05
			1.37		
L-Valine					
IX	6.5	1.57	0.38		0.03
X	6.5	1.64			
XIa	6.5	1.68	1.45		0.07
			1.05		
	11.0	1.69	1.67		0.06
			0.64		
	2.2	1.66	1.24 (2H)		0.06
XIb	6.5	1.64	1.30		0.07
			0.90		
	11.0	1.68	1.34		0.07
			0.92		
	2.2	1.65	1.28		0.07
			0.96		

from the α-carbon of glycine, by ·OH mainly. The reaction of ·OH with amino acids results in hydrogen abstraction from the saturated carbons[31,46–48]:

$$-\overset{|}{\underset{|}{C}}-H + {}^{\cdot}OH \rightarrow -\overset{|}{\underset{|}{C}}{}^{\cdot} + H_2O \qquad (12)$$

Unreacted glycine, detected by using an amino acid analyzer, was eluted near the third peak, for which no substantial ESR signal was observed.

L-Alanine[43]. Separation of the spin adducts produced by irradiation of an aqueous solution of L-alanine (1.0 *M*) containing MNP was performed by use of the same buffer as that used for glycine; two spin adducts originating from L-alanine could be isolated and assigned to structures VII and VIII:

tert.-Bu–N(O•)–CH(CH_3)COO^- VII

tert.-Bu–N(O•)–CH_2–*CH(NH_3^+)COO^- VIII

In structure VIII, the asterisk indicates an asymmetric carbon atom. The h.f.s.c.s obtained are listed in Table II.

Spin adduct VII produced through the reductive deamination of L-alanine by e_{aq}^- showed a reversible pH-dependent shift of the ESR signals. In Fig. 4, the h.f.s.c. for the β-hydrogen atom is plotted against the pH of the solution. Since the interchange between the acid form (A) and the base form (B) of the adduct is rapid, the h.f.s.c. observed in the intermediate pH region is the weighted average of the values for the two forms[49]. By taking the values, a_A and a_B, for each form (see Table II) and using eqn. 13

$$a_{\beta H} = \frac{a_A + a_B \times 10^{pH-pK_a}}{1 + 10^{pH-pK_a}} \tag{13}$$

the variation of $a_{\beta H}$ with pH can be calculated. The pK_a value of adduct VII was determined to be 3.2 by fitting eqn. 13 to the experimental points.

The ESR spectrum of spin adduct VIII consisted of six narrow and six broad lines as depicted in Fig. 5. The intensities of the two types of lines were similar. This ESR pattern is typical of an aminoxyl radical which has an α-methylene group and an asymmetric β-carbon atom, that is, *tert.*-Bu–N(O•)–CH_2–*CXYZ. The characteristic non-equivalence of the two β-hydrogens with linewidth alternation (LWA) has been interpreted by assuming, for example, insufficiently rapid interconversion between the two minimum energy rotamers having mutually different sets of β-H h.f.s.c.s[50]. For spin adduct VIII, a pH titration was carried out to obtain the p$K_{NH_3^+}$ value. The ESR signals arising from the zwitterion form and the anion form overlapped with equal intensities when the interchange between them was slow, yielding a p$K_{NH_3^+}$ value of 8.9.

L-*Valine*[51,52]. A complicated ESR spectrum (Fig. 6a) was obtained upon γ-irradiation of an aqueous 0.07 *M* L-valine solution containing MNP. The overlapping

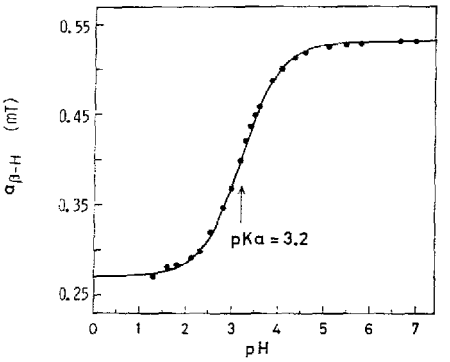

Fig. 4. The effect of pH on the β-H h.f.s.c. for spin adduct VII from L-alanine. Circles indicate experimental results. The best fit solid curve was calculated by use of eqn. 13.

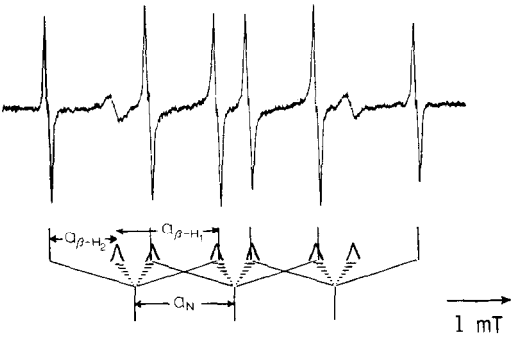

Fig. 5. ESR spectrum and stick diagram of spin adduct VIII from L-alanine (pH 7.0, *ca.* 25°C).

of ESR signals is due to the presence of several spin adducts. By use of a sodium phosphate buffer (150 m*M*, pH 6.5), the ESR and UV chromatograms shown in Fig. 6b were obtained. There are five peaks (A–E) in the ESR chromatogram. Peaks A, C, D and E exhibited ESR spectra shown in Fig. 7 a–d, respectively. The corresponding h.f.s.c.s are listed in Table II. No analyzable ESR spectrum could be obtained for peak B.

Peak A appeared near the void volume and produced an ESR spectrum consisting of 3 × 2 lines (Fig. 7a). The spin adduct was assigned to the structure IX

tert.-Bu–N(O•)–CH(COO$^-$)CH(CH$_3$)$_2$ IX

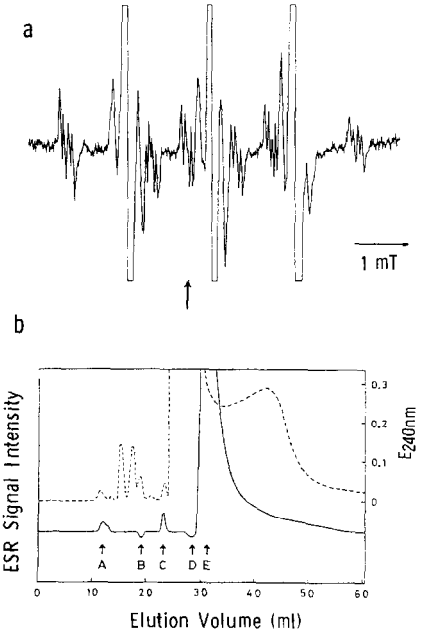

Fig. 6. (a) ESR spectrum of an aqueous solution of L-valine (0.07 *M*) containing MNP immediately after γ-irradiation. During chromatography, the magnetic field was fixed at the position indicated by the vertical arrow. (b) Chromatogram of the solution obtained by UV (broken line) and ESR (solid line) detection. Flow-rate, 0.2 ml/min. Eluent: 0.15 *M* sodium phosphate buffer, pH 6.5.

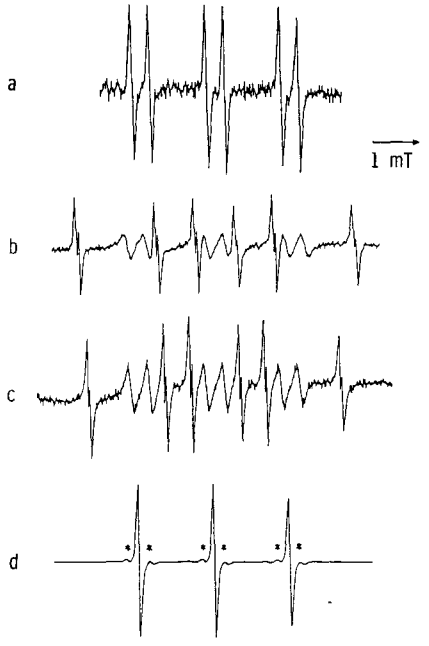

Fig. 7. ESR spectra obtained at pH 6.5 from the fractions giving peaks A (a), C (b), D (c) and E (d) in Fig. 6b. In d the satellite signals (indicated with asterisks) are due to secondary splittings (0.50 mT) caused by an α-^{13}C nucleus.

the parent radical of which was derived through the deamination by e_{aq}^-.

Peak E produced a simple triplet (Fig. 7d) whose h.f.s.c. due to the aminoxyl nitrogen (1.64 mT) is different from those for the adducts obtained by the self-trapping of MNP (1.68 and 1.72 mT). This triplet was identified as due to the adduct produced by hydrogen abstraction by ·OH:

$$\textit{tert.}\text{-Bu–N(O}^{\bullet}\text{)–C(CH}_3\text{)}_2\text{CH(NH}_3^+\text{)COO}^- \qquad \text{X}$$

The six ESR signals labelled with asterisks in Fig. 7d are satellites (splitting 0.50 mT) due to the presence of an α-^{13}C nucleus.

The spectra obtained from peaks C and D produced splitting patterns similar to that of spin adduct VIII from L-alanine. These patterns are characteristic of aminoxyl radicals, *tert.*-Bu–N(O·)–CH_2–C*XYZ[50]. Consequently both peaks C and D were assigned to structure XI

$$\textit{tert.}\text{-Bu–N(O}^{\bullet}\text{)–CH}_2\text{–C*H(CH}_3\text{)C*H(NH}_3^+\text{)COO}^- \qquad \text{XI}$$

i.e., these adducts are a pair of diastereomeric radicals, (*S,S*) and (*R,S*) forms. Isomers XIa and XIb refer to the adducts contained in peaks C and D, respectively. We could not make each isomer XIa and XIb correspond to their individual absolute configuration, the (*S,S*) and (*R,S*) forms. The scheme by which these isomers were formed is represented by:

$$(CH_3)_2CH\text{–}C^*H(NH_3^+)COO^- \xrightarrow{\cdot OH} \cdot CH_2C^*H(CH_3)\text{–}C^*H(NH_3^+)COO^-$$

$$\xrightarrow{MNP} \textit{tert.}\text{-Bu–N(O}\cdot\text{)–}CH_2C^*H(CH_3)\text{–}C^*H(NH_3^+)COO^- \quad (14)$$

(*S*,*S*) and (*R*,*S*) forms

where the diastereoisomerism results from the primary asymmetric centre of L-valine and the new asymmetric centre introduced by hydrogen abstraction from a methyl group in L-valine by ·OH.

The pH-dependent spectral changes for the isomers were observed. Isomer XIa showed a β-H LWA pattern in the form of a triplet at acidic pH, and as a quartet in basic and neutral solutions. The triplet whose central line was broadened indicates that the two β-hydrogens are still non-equivalent. On the other hand, the β-H of isomer XIb produced a four-line LWA pattern at any pH. All the h.f.s.c.s obtained are summarized in Table II. The pK_a values of the isomers could be obtained by changing the pH and simultaneously observing the spectral changes. The $pK_{NH_3^+}$ values were 8.9 and 8.4 for isomers XIa and XIb, respectively.

TABLE III

H.F.S.C.S OF THE SPIN ADDUCTS FROM L-ISOLEUCINE AND L-LEUCINE

Spin adducts	*pH*	*h.f.s.c. (mT)*			
		a_N	$a_{\beta H}$	$a_{\beta N}$	$a_{\gamma H}$
L-*Isoleucine*					
XII	6.0	1.57	0.36		
XIII	6.5	1.64		0.08	
	12.0	1.71			
XIV	6.5	1.62	0.21		
	12.0	1.66	0.31		
XV	7.0	1.69	1.19		0.07 (2H)
			0.98		
XVI	11.5	1.67	1.37		
			0.96		
	7.0	1.60	1.14 (2H)		
XVIIa	6.0	1.59			
XVIIb	6.0	1.61			
L-*Leucine*					
XVIII	6.0	1.58	0.38		0.04 (2H)
VIII	6.5	1.64	2.76* (2H)		
XIX	6.5	1.52			
XX	6.5	1.54			
XXI	10.0	1.69			
XXII	6.5	1.69	1.31		
			1.06		
	11.4	1.69	1.35		
			0.98		

* $a_{H(1)} + a_{H(2)} = 2.76$ mT.

L-*Isoleucine*[53]. The radiolytic decomposition of L-isoleucine in the presence of MNP resulted in a number of spin adducts. The previously mentioned methods of elution did not resolve the peaks in the presence of the excess of unreacted L-isoleucine and the final decomposition products. Therefore, gradient elution was applied. Since the retention volumes of the adducts were found to be highly dependent on the pH of the eluent, the separation could not be achieved by stepwise elution. A linear gradient (90 min) from 0.15 *M* sodium phosphate buffer (pH 6.0) to 0.2 *M* borax–sodium hydroxide buffer (pH 10.0) was applied. Also, isocratic elution with 0.15 *M* phosphate buffer was used in order to isolate the adducts unstable in alkaline solution. Seven different spin adducts could thus be isolated; the corresponding h.f.s.c.s are listed in Table III.

From the fractions obtained by gradient elution, five bands could be detected and 0.3 ml of each fraction was used for further analyses. As expected, from the first peak, the deamino adduct

$$tert.\text{-Bu–N(O}^{\bullet}\text{)–CH(COO}^{-}\text{)CH(CH}_3\text{)C}_2\text{H}_5 \qquad \text{XII}$$

was obtained. This adduct was eluted much more rapidly than the other four.

An ESR spectrum obtained for the second peak consisted of a triplet further split into a triplet with lines of equal intensity. The secondary splitting is attributed to the amino nitrogen, and the adduct was assigned to:

$$tert.\text{-Bu–N(O}^{\bullet}\text{)–C(NH}_3^{+}\text{)(COO}^{-}\text{)CH(CH}_3\text{)C}_2\text{H}_5 \qquad \text{XIII}$$

The amino β-N h.f.s.c. is fairly small compared to values corresponding to the amido nitrogens in the adducts from dipeptides (see Table VI). This type of spin adduct was not observed for the smaller amino acids such as L-alanine and L-valine, which may suggest that the lifetime of aminoxyl radicals from amino acids except glycine is dependent on the size of the adduct.

The spectrum obtained for the third fraction was assigned to the structure:

$$tert.\text{-Bu–N(O}^{\bullet}\text{)–CH(CH}_3\text{)CH(CH}_3\text{)CH(NH}_3^{+}\text{)COO}^{-} \qquad \text{XIV}$$

The fourth fraction contained the spin adduct:

$$tert.\text{-Bu–N(O}^{\bullet}\text{)–CH}_2\text{CH}_2\text{*CH(CH}_3\text{)CH(NH}_3^{+}\text{)COO}^{-} \qquad \text{XV}$$

The ESR spectrum of this adduct comprised a triplet with a secondary splitting into a 1:1:1:1 quartet which was further split into a 1:2:1 triplet. Although in this spin adduct there are two methylene groups between the aminoxyl nitrogen and the asymmetric carbon atom, a four-line splitting pattern due to the two non-equivalent β-hydrogens was observed. By varying the pH of the fractions, it was found that the h.f.s.c.s of adduct XIV, in which there are two carbons between the amino group and the α-carbon, are highly pH-dependent in neutral and basic solutions, while the values for adduct XV, where the α-carbon is three carbons away from the amino group, were almost unchanged. This may indicate the limit of the effect of structural changes in the amino group on the h.f.s.c.s.

The fifth peak gave an ESR spectrum comprised of three sets of four lines when the pH was 11.5, and was assigned to the structure:

tert.-Bu–N(O•)–$CH_2CH(C_2H_5)CH(NH_2)COO^-$ XVI

The four lines, however, were converted into an extremely broad triplet with an intensity ratio of 1:2:1 in neutral solution. This broadening is considered to be unique because it is introduced by the change in the pH.

By the isocratic elution, two simple triplets with the N-h.f.s.c.s different from those of the similar triplets from MNP were obtained. These adducts were characterized as a pair of diastereomers:

tert.-Bu–N(O•)–$*C(CH_3)(C_2H_5)*CH(NH_3^+)COO^-$ XVIIa and XVIIb

These adducts were highly unstable at alkaline pH.

L-*Leucine*[53]. Gradient elution analogous to that used for L-isoleucine was applied and seven different spin adducts were isolated and identified by ESR spectroscopy. All the h.f.s.c.s obtained are summarized in Table III.

The spectrum of the first fraction eluted near the void volume was assigned to the adduct formed via deamination by e_{aq}^-:

tert.-Bu–N(O•)–$CH(COO^-)CH_2CH(CH_3)_2$ XVIII

The second fraction contained the same spin adduct as that (structure VIII) generated from L-alanine. This implies the occurrence of C–C bond scission.

The spectra observed for the third, fourth and sixth fractions each comprised broad triplets, and were tentatively assigned to spin adducts XIX, XX and XXI, respectively:

tert.-Bu–N(O•)–$C(NH_3^+)(COO^-)CH_2CH(CH_3)_2$ XIX

tert.-Bu–N(O•)–$CH[CH(NH_3^+)COO^-]CH(CH_3)_2$ XX

tert.-Bu–N(O•)–$C(CH_3)_2CH_2CH(NH_2)COO^-$ XXI

The seventh fraction produced an ESR spectrum with secondary splitting to a quartet with LWA due to the two non-equivalent β-hydrogens[50]. Consequently the spectrum was assigned to the adduct:

tert.-Bu–N(O•)–$CH_2*CH(CH_3)CH_2*CH(NH_3^+)COO^-$ XXII

The adduct contained in the fifth fraction showed a similar four-line pattern. Both of the adducts in the fifth and seventh peaks showed significant spectral changes upon varying the pH. The adduct in the fifth peak was assigned as a diastereomer of the adduct in the seventh fraction.

DL-Methionine[54,55]. Spin adducts formed upon irradiation of aqueous DL-methionine solution containing MNP were found to be inactivated during the separation with a long column. Therefore, a short cation-exchange column (10 cm × 4 mm I.D., IEX-210SC) was used with 63 m*M* borax–sodium hydroxide buffer (pH 11.5) as eluent. All the h.f.s.c.s obtained from the individual spectra are listed in Table IV.

TABLE IV

H.F.S.C.S OF THE SPIN ADDUCTS FROM DL-METHIONINE, L-GLUTAMINE, L-ASPARAGINE, SODIUM L-GLUTAMATE, SODIUM L-ASPARTATE, L-SERINE, AND L-THREONINE

Spin adduct	*pH*	*h.f.s.c. (mT)*					
		a_N	$a_{\beta H}$	$a_{\beta N}$	$a_{\gamma H}$	$a_{\gamma N}$	$a_{\delta H}$
DL-*Methionine*							
XXIII	11.5	1.56	0.47		0.08 (2H)		
II	11.5	1.73	1.42 (3H)				
XXIV	11.5	1.68	1.12 (2H)		0.10 (2H)		
L-*Glutamine*							
XXV	6.8	1.56	0.47		0.055 (2H)		
XXVI	6.8	1.60		0.10	0.14		
					0.10		
					0.05 (3H, amino)		
	11.0	1.61		0.10	0.135		
					0.10		
XXVII	6.8	1.53	0.40		0.06 (2H)	0.06	0.06 (amide)
	11.0	1.55	0.34		0.07 (2H)	0.07	0.07 (amide)
L-*Asparagine*							
XXVIIIa	1.3	1.51	0.53				
	6.8	1.51	0.41		0.11		
	11.0	1.52	0.33			0.075 (amino or amide)	
							0.075 (amide)
XXVIIIb	6.8	1.51	0.36				
Sodium L-*glutamate*							
XXIX	6.8	1.56	0.45		0.055 (2H)		
XXX	1.6	1.53	0.28				
	6.8	1.57	0.48		0.055 (2H)		
	12.0	1.55	0.44		0.06 (2H)		
Sodium L-*aspartate*							
XXXI	6.8	1.57	0.58		0.06 (2H)		
XXXIIa	1.6	1.50	0.34				
	6.8	1.53	0.39				
	11.0	1.54	0.49				
XXXIIb	1.6	1.52	0.25		0.07		
	6.8	1.57	0.32		0.07		
	11.0	1.56	0.44		0.06		
L-*Serine*							
XXXIII	5.4	1.50	0.17				
XXXIV	1.6	1.54	0.26		0.03 (2H)		
	6.8	1.56	0.44		0.04 (2H)		
L-*Threonine*							
XXXV	1.5	1.53	0.27				
	6.8	1.56	0.42				
XXXVI	6.8	1.63	1.51		0.08		
			0.68				
	11.0	1.65	1.57		0.08		
			0.64				

The first peak was found to contain the deamino adduct from DL-methionine:

tert.-Bu–N(O·)–CH(COO$^-$)$CH_2CH_2SCH_3$ XXIII

The second fraction contained two kinds of adducts. One of the ESR spectra gave three sets of four lines with an intensity ratio of 1:3:3:1 due to adduct II. The other comprised 3 × 3 × 3 lines and was assigned to the adduct:

tert.-Bu–N(O·)–$CH_2CH_2CH(NH_3^+)COO^-$ XXIV

This assignment supports the scheme proposed previously[23]:

$$\begin{aligned} e_{aq}^- + CH_3SCH_2CH_2CH(NH_3^+)COO^- \rightarrow \\ CH_3S^- + {}^{\cdot}CH_2CH_2CH(NH_3^+)COO^- \\ \text{and} \\ {}^{\cdot}CH_3 + {}^-SCH_2CH_2CH(NH_3^+)COO^- \end{aligned} \quad (15)$$

However, spin adducts of S-centered radicals could not be observed in the present work.

L-*Glutamine*[56]. Aqueous L-glutamine solutions irradiated in the presence of MNP produced a highly complex ESR spectrum due to the overlap of the spectra of several spin adducts. For the separation of the adducts, 0.2 *M* phosphate buffer (pH 6.8) was used and five peaks appeared in the ESR chromatogram. The elution volumes of the peaks were 9.8, 14.8, 16.8, 18.0 and 20.5 ml. Analyzable spectra were obtained from the first, third and fifth fractions. The h.f.s.c.s of the three spin adducts are summarized in Table IV.

The ESR spectrum obtained for the first rapidly eluted fraction was not changed at alkaline pH, and was assigned to the deamino adduct from L-glutamine:

tert.-Bu–N(O·)–CH(COO$^-$)$CH_2CH_2CONH_2$ XXV

The ESR spectrum obtained from the third peak was highly complex and consisted of three sets of eleven lines with small h.f.s.c.s. In order to analyze this spectrum, ESR measurements were carried out in water and deuterium oxide. Also the second derivatives of the spectra were obtained. The eleven lines observed in water were converted into ten lines in deuterium oxide, implying that the former spectrum involved hyperfine splittings due to at least one exchangeable hydrogen in the amino group or the amide group of the spin adduct. The spectrum observed in alkaline solutions was different from that in neutral water, revealing that the aminoxyl group is relatively close to the amino group. Based on these results, the spectrum was assigned to the structure:

tert.-Bu–N(O·)–C(NH_3^+)(COO$^-$)$CH_2CH_2CONH_2$ XXVI

This assignment was confirmed by computer simulation of the spectra.

The fifth peak produced an ESR spectrum comprised of a triplet further split into 2 × 6 lines in water and 2 × 5 lines in deuterium oxide. Since it is reasonable

to infer that this spectral change was caused by the change in splittings arising from one of the two exchangeable amide hydrogens, the spin adduct was assigned to the following structure:

tert.-Bu–N(O·)–CH($CONH_2$)$CH_2CH(NH_3^+)COO^-$ XXVII

The ESR parameters used for the simulation of the spectrum in deuterium oxide were the same as those for the spectrum in water except that the h.f.s.c. for the amide hydrogen was replaced by zero.

L-*Asparagine*[56]. The same eluent as that for the L-glutamine system was used for the chromatographic separation of a γ-irradiated aqueous L-asparagine solution, which produced three peaks. The elution volumes of the peaks were 11.9, 19.6 and 27.4 ml.

From the second and third peaks the diastereomeric spin adduct XXVIII could be isolated:

tert.-Bu–N(O·)–*CH($CONH_2$)*CH(NH_3^+)COO^- XXVIII

The secondary splittings of the spectrum of the second fraction gave a relatively broad doublet at pH 6.8 and a doublet of quartets at pH 11.0 in water, a doublet at pH 6.8 and a doublet of triplet at pH 11.0 in deuterium oxide. All the h.f.s.c.s obtained for the isomers are summarized in Table IV.

Sodium L-*glutamate*[56]. The γ-irradiated aqueous solution of sodium L-glutamate containing MNP yielded two rapidly eluted peaks (elution volumes: 10.1 and 10.6 ml) due to the existence of two carboxyl groups in the adduct. A flow-rate of 0.1 ml/min was used for the separation.

The spectrum of the first fraction comprised of 3 × 2 × 3 lines and was assigned to the deamino adduct:

tert.-Bu–N(O·)–CH(COO^-)$CH_2CH_2COO^-$ XXIX

From the second fraction, a triplet of doublets was obtained. By observation of the changes in h.f.s.c.s upon varying the pH (see Table IV), this spectrum was assigned to the spin adduct:

tert.-Bu–N(O·)–CH(COO^-)$CH_2CH(NH_3^+)COO^-$ XXX

All the h.f.s.c.s are listed in Table IV.

Sodium L-aspartate[56]. The chromatographic conditions for the separation of the adducts from sodium L-aspartate were the same as those used for sodium L-glutamate. From the first band (elution volume: 10.9 ml), the spin adduct XXXI could be isolated:

tert.-Bu–N(O·)–CH(COO^-)CH_2COO^- XXXI

The spin adducts from the second and third fractions were found to be a pair of diastereomeric radicals:

tert.-Bu–N(O·)–*CH(COO$^-$)*CH(NH_3^+)COO$^-$ XXXII

The detailed assignment of both spectra was performed by changing the solvent to deuterium oxide. The h.f.s.c.s of the three adducts are summarized in Table IV.

L-*Serine*[56]. The major component of the ESR spectrum obtained immediately after radiolysis of an aqueous L-serine solution containing MNP consisted of 3 × 2 lines and was assigned to the structure:

tert.-Bu–N(O·)–CH(OH)CH(NH_3^+)COO$^-$ XXXIII

The chromatographic separation of the sample under the same conditions as those used for the L-glutamine system yielded a species exhibiting a spectrum comprised of 3 × 2 × 3 lines which was assigned to the structure:

tert.-Bu–N(O·)–CH(COO$^-$)CH_2OH XXXIV

The h.f.s.c.s obtained are shown in Table IV.

L-*Threonine*[56]. The chromatographic analysis of an irradiated aqueous solution containing L-threonine and MNP, under the same conditions as those used for the L-glutamine system, yielded two spin adducts. The spin adduct contained in the first fraction was assigned to the structure:

tert.-Bu–N(O·)–CH(COO$^-$)CH(OH)CH_3 XXXV

From the second peak, an ESR spectrum consisting of 3 × 4 lines with LWA was obtained and assigned to the adduct:

tert.-Bu–N(O·)–CH_2*CH(OH)*CH(NH_3^+)COO$^-$ XXXVI

The h.f.s.c.s of these two adducts are listed in Table IV.

Separation of spin adducts from L-*proline and its 4-substituted derivatives*[57,58]

L-*Proline and cis-4-chloro*-L-*proline*. An aqueous solution containing L-proline (Pro) and MNP, cooled in an ice-bath, was γ-irradiated with a total dose of 3 kGy. The ESR spectrum of this solution just after γ-irradiation is shown in Fig. 8a. Chromatography of the solution with ESR detection gave six peaks (A–F) as shown in Fig. 9a. The fraction corresponding to peak A gave no ESR signals. The ESR spectrum obtained from the fraction corresponding to peak D was complex, and a satisfactory identification could not be made. Fig. 10a–d shows ESR spectra obtained from the fractions corresponding to peaks B, C, E and F, respectively. Most of the spin adducts produced by self-trapping of MNP[37,38] were adsorbed on the column and eluted very slowly.

Fig. 10a shows the ESR spectrum obtained for peak B at pH 7. At pH 11.4 the spectral pattern showed little change. The h.f.s.c.s are given in Table V. Whereas the deamino adducts originating from the attack of e_{aq}^- on amino acids are excluded when chromatographed using a cation-exchange column with neutral eluents, as described above, the spin adduct found here is not excluded under these chromato-

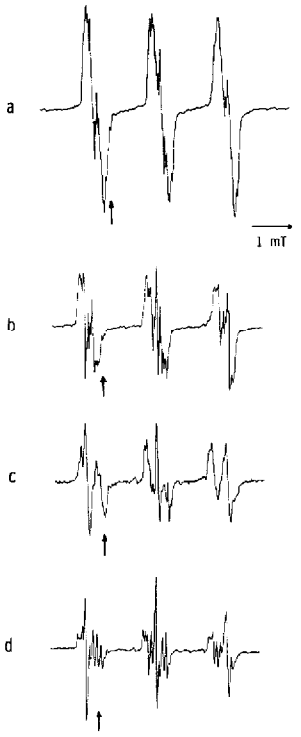

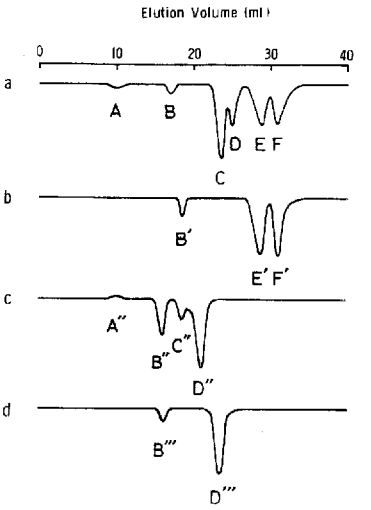

Fig. 8. ESR spectra of γ-irradiated aqueous solutions of 0.2 *M* Pro (a), 0.1 *M* Cl-Pro and 0.3 *M* sodium formate (b), 0.2 *M* *trans*-4-Hyp (c) and 0.2 *M* *cis*-4-Hyp containing 5 mg/ml MNP (d). During chromatography, the magnetic fields were fixed at the positions indicated by the vertical arrows.

Fig. 9. Chromatograms of γ-irradiated aqueous solutions containing MNP obtained by ESR detection: Pro (a); Cl-Pro with sodium formate (b); *trans*-4-Hyp (c); *cis*-4-Hyp (d). The units of the vertical axes represent relative ESR signal intensities. The chromatographic conditions were as follows: column, IEX-210SC (Toyo Soda, 60 × 0.75 cm); pressure, *ca.* 70 kg/cm²; flow-rate, *ca.* 0.2 ml/min; temperature, *ca.* 25°C. The column was first equilibrated with 0.2 *M* sodium phosphate buffer (pH 6.8). After the sample injection, a 90-min gradient (X^4 mode, Gradient Device GE-2, Toyo Soda) was started: 0.2 *M* sodium phosphate buffer (pH 6.8) to 0.2 *M* Na_2HPO_4–NaOH buffer (pH 11.5).

graphic conditions, which suggests that the adduct is not negatively charged. Consequently, the spin adduct was assigned as the cleavage adduct from L-proline, with the structure:

$$tert.\text{-Bu–N(O·)–CH(COO}^-\text{)CH}_2\text{CH}_2\text{CH}_2\text{NH}_3^+ \qquad \text{XXXVII}$$

Spin adduct XXXVII originates from reductive cleavage of the pyrrolidine ring induced by the addition of a hydrated electron to the carboxyl group[31,44].

Computer simulations of the ESR spectra of fraction C in water (Fig. 10b) and deuterium oxide were conducted. The parameters estimated are shown in Table V. On the basis that the adduct has observable h.f.s.c.s for a β-hydrogen and a β-nitrogen atom, it was assigned to the structure XXXVIII,

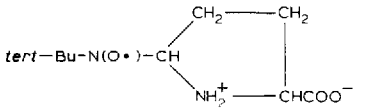

XXXVIII

which is the Pro C-5 adduct arising from hydrogen abstraction from the C-5 position by a hydroxyl radical.

Fig. 10c and d shows the ESR spectra for the fractions corresponding to peaks E and F, respectively. Computer simulations were conducted for solutions in both water and deuterium oxide, and the parameters estimated are shown in Table V.

In order to identify the spin adducts more reliably, the Pro C-4 adduct

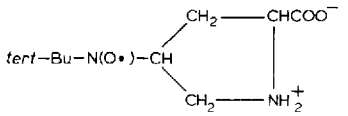

XXXIX

was produced as follows. The spin-trapping and HPLC–ESR techniques were applied to a γ-irradiated aqueous solution of *cis*-4-chloro-L-proline (Cl-Pro) contain-

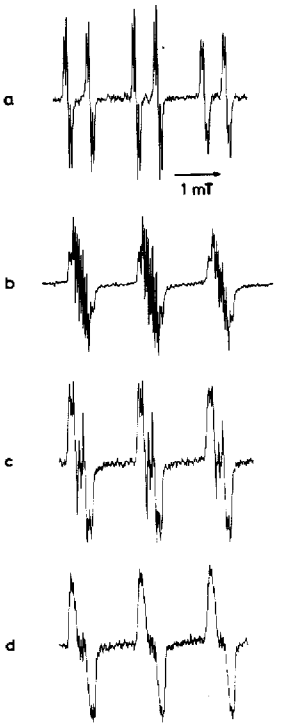

Fig. 10. ESR spectra (a–d) (pH 7, water) obtained from the fractions giving peaks B, C, E and F respectively in Fig. 9a.

TABLE V

H.F.S.C.S OF THE SPIN ADDUCTS FROM L-PROLINE AND 4-SUBSTITUTED L-PROLINE

Spin adduct	*Peak*[a]	*pH*	*h.f.s.c. (mT)*					ΔH_{pp}[b]	*Ratio*[c]
			a_N	$a_{\beta H}$	$a_{\beta N}$	$a_{\gamma H}$	$a_{\delta H}$		
XXXVII	B	7	1.56	0.50		0.05 (2H)			
		11	1.57	0.49		0.05 (2H)			
XXXVIII	C	7	1.60	0.23	0.046	0.092 (2H)			
						0.04[d]			
						(0.006)[e]		0.030	
XXXIXa[f]	E, E′	7	1.61	0.21		0.09	0.035[d]	0.031	
						0.085	(0.0055)[e]		
						0.04			
						0.03			
XXXIXb[f]	F, F′	7	1.60	0.20		0.10	0.035[d]	0.030	
						0.09	(0.0055)[e]		
						0.05	0.03		
						0.045			
XL	B′	7	1.55	0.50		0.06 (2H)			
		11	1.55	0.47		0.06 (2H)			
XLI[g]	B″	7	1.57	0.49		0.05 (2H)			
		11	1.57	0.46		0.05 (2H)			
	B‴	7	1.56	0.49		0.06 (2H)			
		11	1.57	0.45		0.06 (2H)			
XLII[h]	D″	7	1.53	0.255	0.085	0.085		0.050	
						0.03[d]			
						(0.0045)[e]			
			1.53	0.255	0.06	0.06		0.050	2/1[i]
						0.03[d]			
						(0.0045)[e]			
	D‴	7	1.56	0.255	0.085	0.085		0.035	
						0.025[d]			
						(0.004)[e]			
			1.56	0.255	0.10	0.10		0.035	3/1[i]
						0.025[d]			
						(0.004)[e]			

[a] Chromatographic peak in Fig. 9.
[b] Lorentzian peak-to-peak linewidth (mT) used for spectrum simulation.
[c] Concentration ratio for spectrum simulation: upper set/lower set.
[d] NH hydrogen convertible into ND deuterium in ^2H_2O.
[e] a_D(ND) value in ^2H_2O.
[f] XXXIXa and XXXIXb correspond to the *cis* and *trans* isomers, respectively. For further details about the isomers see the text.
[g] Each fraction giving peaks B″ and B‴ was a mixture of a pair of diastereomeric adducts. All h.f.s.c.s are the average of the values of the two diastereoisomers. Each adduct from peak B″ is the enantiomer of either adduct from peak B‴.
[h] Each fraction giving peaks D″ and D‴ was a mixture of a pair of epimeric adducts. Each adduct from peak D″ is also epimeric for either adduct from peak D‴ with respect to the C-4 position.
[i] The coexisting epimeric adducts from peaks D″ or D‴ have the same g values.

ing sodium formate, which reacts with $^{\cdot}OH$[59]:

$$^{\cdot}OH + HCOO^- \rightarrow H_2O + {}^{\cdot}COO^- \qquad (16)$$

Pro C-4 adducts are derived from the selective dechlorination by $^{\cdot}COO^{-}$[59]:

$$-\overset{|}{\underset{|}{C}}-Cl + {}^{\cdot}COO^{-} \rightarrow -\overset{|}{\underset{|}{C}}{}^{\cdot} + Cl^{-} + CO_2 \qquad (17)$$

Figs. 8b and 9b show the ESR spectrum and the chromatogram of a γ-irradiated aqueous Cl-Pro solution containing sodium formate and MNP. The ESR chromatogram gave three peaks (B′, E′ and F′) as shown in Fig. 9b. In the absence of sodium formate, peaks E′ and F′ were not observed. Typical ESR spectra for the fractions corresponding to peaks B′, E′ and F′ are depicted in Fig. 11a–c.

The spin adduct of peak B′, which produces the ESR spectrum shown in Fig. 11a, was assigned to the structure

tert.-Bu–N(O·)–*CH(COO^{-})–CH_2–*CHCl–$CH_2NH_3^{+}$ XL

the cleavage adduct from Cl-Pro, on the basis that its hyperfine structure (h.f.s.) and elution position are very similar to those of adduct XXXVII from L-proline. It is concluded that peak B′ comprises a mixture of the diastereomers XL having very similar ESR parameters[60].

Fig. 11b and c shows the ESR spectra for the fractions corresponding to peaks

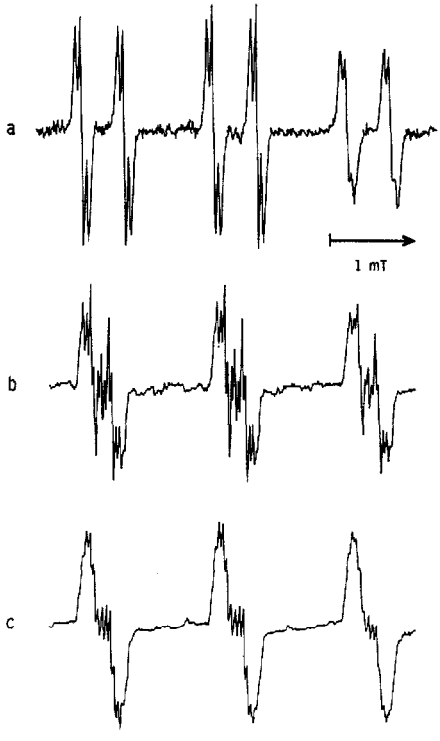

Fig. 11. ESR spectra (a–c) (pH 7, water) obtained from the fractions giving peaks B′, E′ and F′ respectively in Fig. 9b.

E′ and F′, respectively. Their retention times and spectral patterns are virtually identical with those of peaks E and F of the Pro system (Fig. 9a). Since sodium formate was essential for the observation of peaks E′ and F′, as stated above, both spin adducts were assigned the structure XXXIX, *i.e.*, a pair of the diastereomeric Pro C-4 adducts, which originate from the dechlorination of the C-4 position in Cl-Pro by $\cdot COO^-$ (eqn. 17)[59]. The two possible absolute configurations of spin adducts XXXIX are the *cis*- and *trans*-isomers

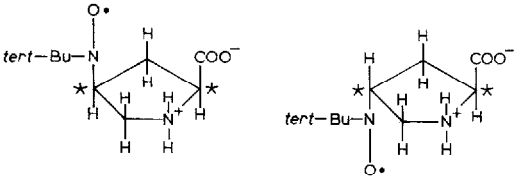

XXXIX a XXXIX b

with respect to the carboxyl and the *tert.*-butyl aminoxyl groups in the pyrrolidine rings. The absolute configurations of the isomers from peaks E and E′ and from F and F′ were examined. The so-called "W-plan" (2 V) for spin transmission through σ bonds is the most important empirical concept used for explaining the stereoselectivity of long-range h.f.s.c.s[61]. The relationship between the δ-H h.f.s.c.s given in Table V and the minimum energy conformations for the *cis*- and *trans*-isomers was considered in terms of the extended W-plan (2.5 V, *i.e.* ⟍⟍) arrangement. Consequently, it is suggested that the diastereomer from peaks E and E′ corresponds to configuration XXXIXa (*cis*) and that from F and F′ to XXXIXb (*trans*).

*trans- and cis-4-Hydroxy-*L*-proline.* Figs. 8c and 9c show the ESR spectrum and the chromatogram of a γ-irradiated aqueous solution of *trans*-4-hydroxy-L-proline (*trans*-4-Hyp) containing MNP. The ESR chromatogram contained four peaks (A″–D″) as shown in Fig. 9c. The fraction corresponding to peak A″ did not give any signals, and peak C″ did not contain a sufficient amount of the spin adduct for analysis.

Figs. 8d and 9d show the ESR spectrum and the chromatogram of the *cis*-4-hydroxy-L-proline (*cis*-4-Hyp) system. The chromatogram exhibited two peaks (B‴ and D‴) as shown in Fig. 9d.

The retention time and ESR spectrum of peak B″ are virtually identical with those of peak B‴. These peaks were thus assigned to the cleavage adduct from *trans*- and *cis*-4-Hyp, respectively:

$$tert.\text{-Bu–N(O}\cdot\text{)–*CH(COO}^-\text{)–CH}_2\text{–*CH(OH)–CH}_2\text{NH}_3^+ \qquad \text{XLI}$$

The partial distortion found in the ESR spectrum of peak B″ suggests the coexistence of a pair of diastereomeric adducts, *R,R* and *S,R* forms, whose enantiomers (*S,S* and *R,S* forms, respectively) were obtained from peak B‴. The average h.f.s.c.s at pH 7 and 11 are summarized in Table V.

The ESR spectrum corresponding to peak D″ resembles that for peak D‴. Computer simulations of the spectra were conducted by assuming that each of the fractions is a mixture of two kinds of radicals having slightly different ESR parameters. The ESR parameters estimated from the simulations are summarized in Table V. All of these four spin adducts were assigned the structure:

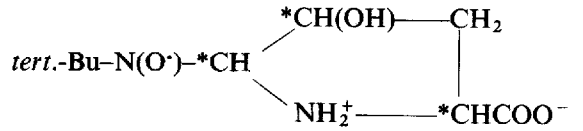

XLII

The two adducts in peak D″ were regarded as a pair of diastereomeric C-5 adducts from *trans*-4-Hyp arising from hydrogen abstractions from the C-5 positions by hydroxyl radicals[31]. The two adducts mixed in peak D‴ were regarded as a pair of epimeric C-5 adducts from *cis*-4-Hyp, each of which is also epimeric for either of the C-5 adducts from *trans*-4-Hyp as regards the C-4 positions whose asymmetric centres are different from each other.

The h.f.s.c.s of the spin adducts formed upon γ-irradiation of aqueous solutions of L-proline and its 4-substituted derivatives containing MNP are summarized in Table V. The spin adducts XXXVII, XL and XLI (cleavage adducts) are derived from reductive cleavages of the pyrrolidine rings induced by the addition of hydrated electrons to the carboxyl groups[31,44]:

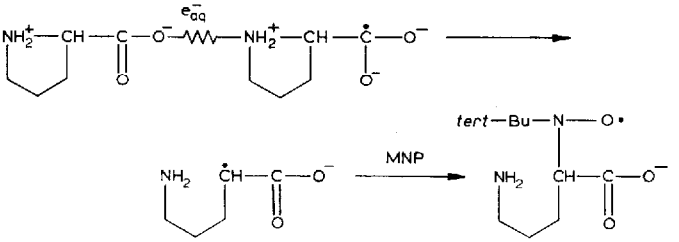

(18)

The C-4 (XXXIX) and C-5 (XXXVIII and XLII) adducts are derived from short-lived radicals produced by hydrogen abstraction from the carbons of the saturated alkyl groups by hydroxyl radicals.

Separation of spin adducts from dipeptides[62,63]

Aqueous solutions of four dipeptides, glycylglycine (Gly-Gly), glycyl-L-alanine (Gly-L-Ala), L-alanylglycine (L-Ala-Gly) and L-alanyl-L-alanine (L-Ala-L-Ala), were γ-irradiated at a dose rate of 0.1 kGy/min with a total dose of 3 kGy in the presence of 5 mg/ml MNP. The concentration of the dipeptides was 0.1 *M*. The irradiated solutions were chromatographed by stepwise elution with two buffers.

Glycylglycine[62]. A 0.25 *M* sodium phosphate buffer, pH 6.0, and 0.2 *M* Na_2HPO_4–NaOH, pH 11.5, were used as the first and the second eluents, respectively, and were switched at the elution volume of *ca.* 30 ml. In the ESR chromatogram of the γ-irradiated Gly-Gly solution, two peaks were eluted at 12.4 and 17.6 ml, and the corresponding fractions gave characteristic ESR spectral patterns.

The spin adduct in the first peak was assigned to the deamino adduct from Gly-Gly:

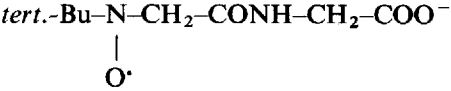

XLIII

The ESR pattern at pH 6.0 obtained for the second peak suggests the formation of a spin adduct having a component *tert.*-Bu–N(O•)–CH–N<:

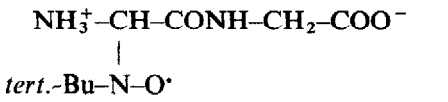

XLIV

or

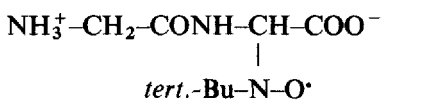

XLV

Whereas in neutral and alkaline solutions the ESR pattern was independent of pH, in the acidic pH range the signals due to the spin adduct exhibited reversible pH-dependent shifts. These changes are mainly due to an increase in the β-h.f.s.c. differences. From the observation of such reversible pH effects, the spin adduct was assigned not to structure XLIV but to XLV, that is, the C-terminal backbone adduct from Gly-Gly. The h.f.s.c.s are given in Table VI. The pK_{COOH} value has been determined to be 2.0 from a plot of the pH dependence of Δa_β ($= a_{\beta N} - a_{\beta H}$)

$$\Delta a_\beta = \frac{\Delta a_\beta^A + \Delta a_\beta^B \times 10^{pH-pK_a}}{1 + 10^{pH-pK_a}} \tag{19}$$

where $\Delta a_\beta^A = 0.11$ mT and $\Delta a_\beta^B = 0.02$ mT for the acid form and the base form, respectively.

Glycyl-L-alanine[62] A 0.1 *M* sodium phosphate buffer, pH 6.0, and 0.2 *M* Na_2HPO_4–NaOH buffer, pH 11.5, were used as the first and the second eluents, respectively, and were switched at the elution volume of *ca.* 24 ml. In the ESR chromatogram of a γ-irradiated Gly-L-Ala solution containing MNP, three peaks were eluted at 11.4, 14.4 and 25.6 ml. The spin adducts of the first, second and third peaks were assigned to the deamino adduct (structure XLVI), the C-terminal backbone adduct (XLVII) and the side-chain adduct (XLVIII) from Gly-L-Ala, respectively:

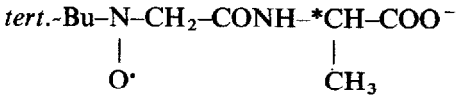

XLVI

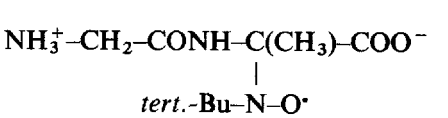

XLVII

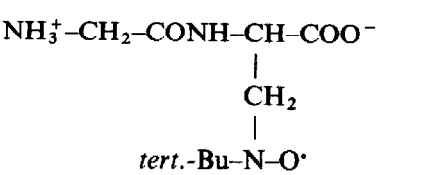

XLVIII

TABLE VI

H.F.S.C.S OF THE SPIN ADDUCTS FROM DIPEPTIDES

Spin adduct	*pH*	*h.f.s.c. (mT)*				
		a_N	$a_{\beta H}$	$a_{\beta N}$	$a_{\gamma H}$	$a_{\gamma N}$
Gly-Gly						
XLIII	6.0	1.59	0.91 (2H)			
XLV	1.0	1.52	0.16	0.26		
	6.0	1.56	0.22	0.24		
Gly-L-*Ala*						
XLVI	6.0	1.60	1.00			
			0.82			
XLVII	6.0	1.52		0.34	0.03 (13H)	
XLVIII	2.0	1.64	1.37 (2H)		0.07	
	6.0	1.64	1.46		0.07	
			0.97			
	8.4	1.64	1.42		0.07	
			0.99			
	12.2	1.64	1.39		0.07	
			1.01			
L-*Ala-Gly*						
XLIX	6.0	1.58	0.33		0.047 (3H)	0.047
La	0.8	1.52	0.160	0.260		
	6.0	1.55	0.233	0.233		
	11.2	1.57	0.215	0.235		
Lb	0.8	1.53	0.150	0.270		
	6.0	1.56	0.193	0.258		
	11.3	1.58	0.205	0.245		
LI	2.0	1.62	1.53		0.05	
			1.18			
	5.9	1.62	*		0.05	
	8.0	1.65	1.26 (2H)		0.07	
L-*Ala*-L-*Ala*						
LIIa	6.0	1.575	0.385		0.045 (3H)	0.045
LIIb	6.0	1.580	0.365		0.050 (3H)	0.050
LIIIa	6.0	1.53		0.339	0.034 (10H)	
LIIIb	6.0	1.52		0.350	0.032 (13H)	
LIV	1.0	1.65	1.39 (2H)		0.07	
	6.1	1.64	1.43		0.07	
			0.99			
	7.9	1.64	1.40		0.07	
			1.01			
	12.4	1.63	1.36		0.07	
			1.05			
LV	7.9	1.65	1.28 (2H)		0.07	

* The two β-hydrogens were presumably non-equivalent ($\Sigma a_{\beta H}$ = 2.63 mT).

Their h.f.s.c.s are given in Table VI.

It was found that spin adduct XLVI exhibits ESR spectra with unequal splittings for the two β hydrogens, while spin adduct XLIII does not. It has already been

known that in the aminoxyl radical *tert.*-Bu–N(O·)–CH_2–*CXYZ the asymmetry of the β-carbon causes unequal splittings for the two β-hydrogens[50]. In the present case the spectrum of spin adduct XLVI revealed that in the aminoxyl radical *tert.*-Bu–N(O·)–CH_2–CONH–*CXYZ even the assymetry of the δ-carbon causes unequal splittings for the two β-hydrogens through the peptide bond. The ESR spectra of spin adduct XLVIII changed remarkably with pH through the acid-dissociation equilibria of the carboxyl or amino group. The pK_a value for the carboxyl group of adduct XLVIII has been determined to be 3.0.

L-*Alanylglycine*[63]. A 0.15 *M* sodium phosphate buffer, pH 6.0, and 0.2 *M* Na_2HPO_4–NaOH, pH 11.5, were used as the first and the second eluents, respectively, and were switched at the elution volume of *ca.* 31 ml. The ESR chromatogram of a γ-irradiated aqueous L-Ala-Gly solution containing MNP exhibited four peaks, eluted at 11.5, 17.0, 19.5 and 33.0 ml. The spin adducts of the first, second, third and fourth peaks were assigned to the deamino adduct (XLIX), the C-terminal backbone adducts (La and Lb) and the side-chain adduct (LI) from L-Ala-Gly, respectively:

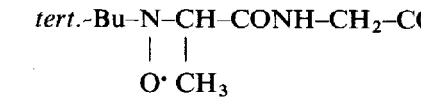

XLIX

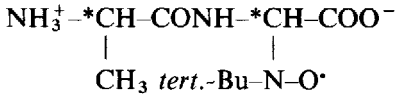

La and Lb

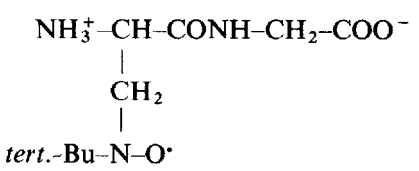

LI

Spin adducts La and Lb are interpreted as a pair of diastereomeric radicals, *S,S* and *S,R* forms, involving the primary asymmetric centre of the L-alanine residue and a new asymmetric centre formed by the addition of MNP to the short-lived radical. Upon separation the individual diastereomeric radicals revealed mutually different h.f.s.c.s (Table VI). Their ESR spectra changed remarkably with pH through the acid-dissociation equilibria of the carboxyl groups. By the use of eqn. 19, the pK_a values have been determined to be 1.8 and 1.6 for the carboxyl groups of adduct La and Lb, respectively.

L-*Alanyl*-L-*alanine*[63]. When a 0.15 *M* sodium phosphate buffer, pH 6.0, and the 0.2 *M* H_3BO_3 · NaCl–NaOH buffer, pH 9.0, were used as the first and the second eluents, respectively, and were switched at *ca.* 33 ml, four peaks were eluted at 11.5, 15.3, 16.8 and 37.0 ml in the ESR chromatogram of a γ-irradiated aqueous L-Ala-L-Ala solution containing MNP.

By computer simulation of the ESR spectrum, the first peak fraction was interpreted to be a (1:1) mixture of a pair of diastereomeric deamino adducts (LIIa and LIIb), *S,S* and *R,S* forms:

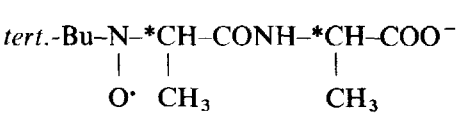
LIIa andLIIb

The spin adducts of the second, third and fourth peaks were assigned to a pair of diastereomeric C-terminal backbone adducts (LIIIa and LIIIb), and the C-terminal side-chain adduct (LIV) from L-Ala-L-Ala, respectively:

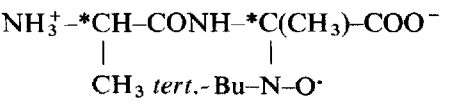
LIIIa and LIIIb

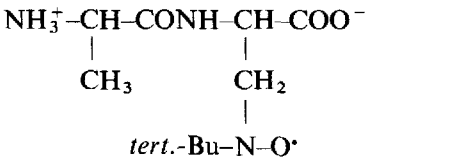
LIV

When sodium phosphate buffers of 0.05 *M*, pH 6.0, and 0.1 *M*, pH 8.0, were used as the first and second eluents, respectively, the N-terminal side-chain adduct

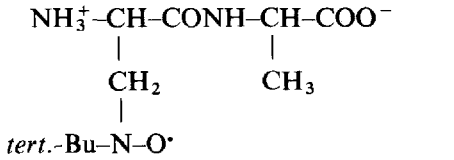
LV

from L-Ala-L-Ala was found in the fraction of pH 7.9.

The h.f.s.c.s of the spin adducts formed upon γ-irradiation of aqueous solutions of Gly-Gly, Gly-L-Ala, L-Ala-Gly and L-Ala-L-Ala containing MNP are summarized in Table VI. The observed γ-h.f.s. for the spin adducts XLVII, LIIIa and LIIIb contained the nine γ-hydrogens in the *tert.*-butyl group arising from MNP. The γ-H hyperfine splittings due to the *tert.*-butyl group are rarely observable. The pH-dependent spectral changes for the side-chain adducts from the dipeptides (XLVIII, LI, LIV and LV) suggest that, in an aqueous solution of *tert.*-Bu–N(O·)–CH_2–*CXYZ, the function of the β asymmetric centre which makes the methylene hydrogens non-equivalent[50] is enhanced by electric charges in proximity to it. It appears from the electron-withdrawing character of the aminoxyl group that the determined pK_{COOH} values of spin adducts VII, XLV, La and Lb are lower than those of the compounds in which the *tert.*-butyl aminoxyl groups of the adducts are substituted by hydrogens.

Separation of spin adducts from tripeptides[64]

Aqueous solutions of four tripeptides (0.1 *M*), Gly-Gly-Gly, Gly-Gly-L-Ala, Gly-L-Ala-Gly and L-Ala-Gly-Gly, were γ-irradiated at a dose rate of *ca.* 75 Gy/min with a total dose of 3 kGy in the presence of 5 mg/ml MNP.

Glycylglycylglycine. A 0.25 *M* sodium phosphate buffer, pH 6.0, and 0.2 *M*

Na_2HPO_4–NaOH buffer, pH 11.5, were used as the first and the second eluents, respectively, and were switched at the elution volume of *ca.* 31 ml. In the ESR chromatogram of the irradiated Gly-Gly-Gly solution, three peaks were eluted at 11.9, 18.1 and 20.0 ml. The spin adducts of the first, second and third peaks were assigned to the deamino adduct (structure LVI), the C-terminal backbone adduct (LVII) and the internal backbone adduct (LVIII) from Gly-Gly-Gly, respectively:

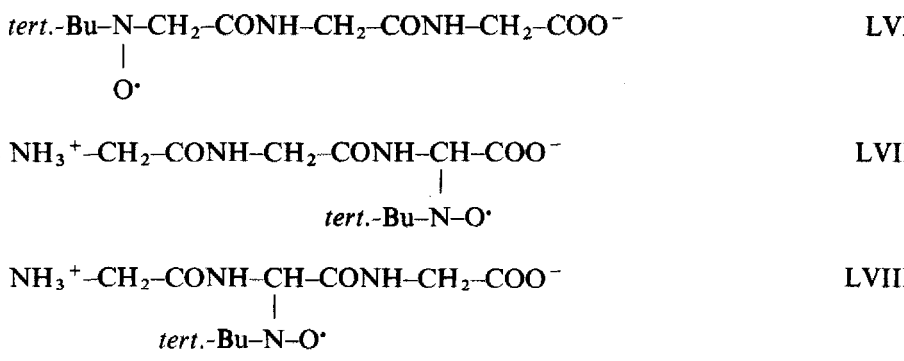

*Glycylglycyl-*L*-alanine.* Fig. 12 shows the ESR spectrum and chromatogram of a γ-irradiated aqueous Gly-Gly-L-Ala solution containing MNP. The ESR chromatogram exhibited four peaks (A–D) as shown by the solid line in Fig. 12b. Typical

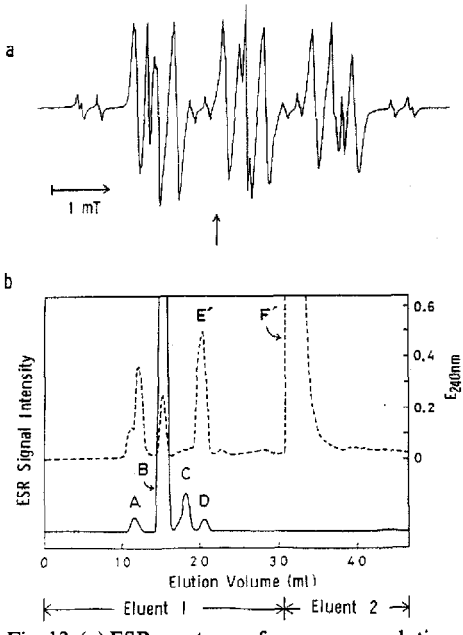

Fig. 12. (a) ESR spectrum of an aqueous solution of Gly-Gly-L-Ala containing MNP observed immediately after γ-irradiation (at pH 5.7). During chromatography, the magnetic field was fixed at the position indicated by the vertical arrow. (b) Chromatogram of the solution obtained by UV (broken line) and ESR (solid line) detection. Flow-rate: *ca.* 0.2 ml/min. Eluents: 1, 0.25 *M* sodium phosphate buffer, pH 6.0; 2, 0.2 *M* Na_2HPO_4–NaOH buffer, pH 11.5.

ESR spectra for the fractions corresponding to peaks A–D are depicted in Fig. 13a–d. Most spin adducts produced by the self-trapping of MNP[37,38] were adsorbed on the column and eluted very slowly with diffusion. In the UV chromatogram shown as the broken line in Fig. 12b, peak E′ is due to unreacted Gly-Gly-L-Ala, detected by using an amino acid analyzer, and peak F′ mainly due to *tert.*-butylnitrosohydroxylamine, *tert.*-BuN(OH)N=O, characterized by the pH dependence of the UV spectra[34,35].

Fig. 13a shows the ESR spectrum (modulation amplitude 0.05 mT) obtained for peak A, and the h.f.s.c.s are given in Table VII. The spin adduct was assigned the structure

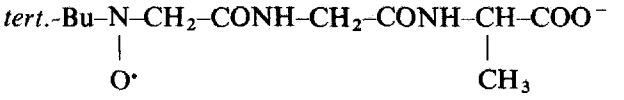

LIX

the deamino adduct from Gly-Gly-L-Ala.

Fig. 13b shows the ESR spectrum for peak B, which is apparently a major component of the ESR spectrum in Fig. 12a. This ESR pattern was assigned the structure

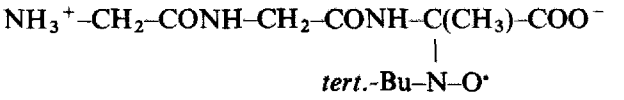

LX

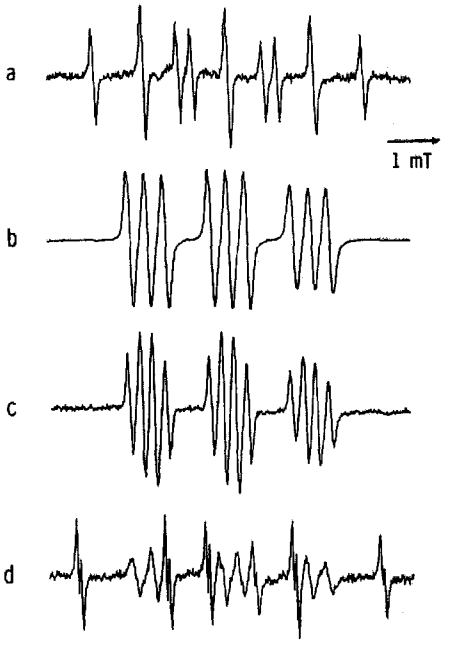

Fig. 13. ESR spectra (a–d) obtained from the fractions giving peaks A–D respectively in Fig. 12b. pH 5.9 (a and d); 6.0 (b and c).

TABLE VII

H.F.S.C.S OF THE SPIN ADDUCTS FROM TRIPEPTIDES

Spin adduct	*pH*	*h.f.s.c. (mT)*				
		a_N	$a_{\beta H}$	$a_{\beta N}$	$a_{\gamma H}$	$a_{\gamma N}$
Gly-Gly-Gly						
LVI	6.0	1.58	0.92 (2H)			0.03
LVII	0.6	1.52	0.16	0.255		
	6.0	1.56	0.20	0.24		
	11.1	1.59	0.20	0.26		
LVIII	0.7	1.50	0.21	0.235		
	6.3	1.51	0.20	0.24		
	11.2	1.53	0.20	0.23		
Gly-Gly-L-Ala						
LIX	5.9	1.59	0.92 (2H)			0.03
LX	6.0	1.52		0.33		
LXI*	1.0	1.51	0.27	0.22		
	6.0	1.51	0.25	0.22		
	12.0	1.53	0.25	0.22		
LXII	5.9	1.63	1.36		0.07	
			1.02			
Gly-L-Ala-Gly						
LXIII	6.0	1.59	0.95			0.03
			0.89			
LXIVa**	0.6	1.52	0.16	0.265		
	6.0	1.54	0.20	0.24		
	11.3	1.56	0.21	0.245		
LXIVb**	0.6	1.52	0.155	0.255		
	6.0	1.55	0.20	0.24		
	11.1	1.56	0.21	0.24		
LXV	0.4	1.46		0.31		
LXVI	6.1	***	***		0.06	
L-Ala-Gly-Gly						
LXVII	5.7	1.56	0.33		0.045 (3H)	0.045
LXVIII*	0.4	1.52	0.15	0.255		
	6.0	1.55	0.21	0.24		
	11.5	1.56	0.205	0.245		
LXIX*	0.5	1.50	0.22	0.24		
	6.0	1.51	0.19	0.24		
	11.7	1.52	0.20	0.23		
LXX	6.6	1.64	1.33§		0.06	

* All h.f.s.c.s are the average values of two diastereoisomers.
** LXIVa and LXIVb are a pair of diastereomeric adducts which were separated.
*** $2a_N + a_{\beta H1} + a_{\beta H2} = 5.78$ mT.
§ Average value for two hydrogens.

the C-terminal backbone adduct from Gly-Gly-L-Ala.

Fig. 13c shows the ESR spectrum for peak C. The spectral pattern was almost pH-independent. The spin adduct was assigned the structure

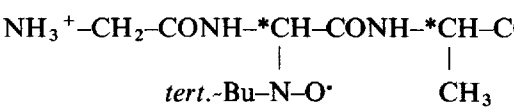

LXI

the internal backbone adduct from Gly-Gly-L-Ala.

Fig. 13d shows the ESR spectrum for peak D, which apparently exhibited a mixture of six narrow and six broad lines. Such a spectrum is typical of an aminoxyl radical, *tert.*-BuN(O·)–CH_2–*CXYZ[50]. The spin adduct was assigned the structure

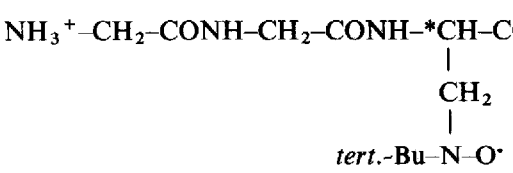

LXII

the side-chain adduct from Gly-Gly-L-Ala.

Glycyl-L-alanylglycine and L-alanylglycylglycine. γ-Irradiated aqueous solutions of Gly-L-Ala-Gly and L-Ala-Gly-Gly were also analyzed under analogous conditions by the HPLC–ESR method. From the irradiated Gly-L-Ala-Gly solution, the deamino adduct (structure LXIII), the C-terminal backbone adducts (LXIVa and LXIVb), the internal backbone adduct (LXV) and the side-chain adduct (LXVI) were identified:

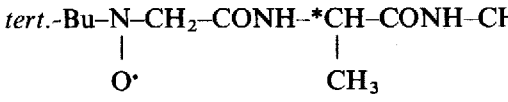

LXIII

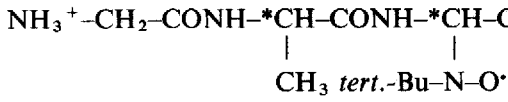

LXIVa and LXIVb

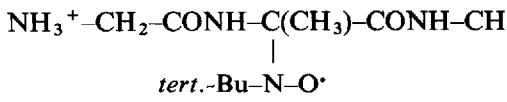

LXV

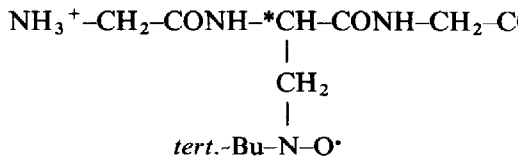

LXVI

The pair of diastereomeric adducts, LXIVa and LXIVb, were separated from each other. From the irradiated L-Ala-Gly-Gly solutions, four spin adducts were identified:

LXVII

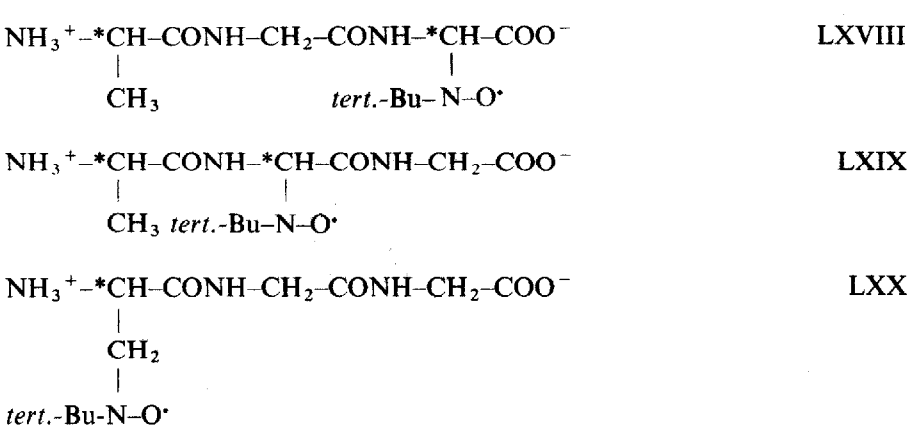

LXVIII

LXIX

LXX

Spin-trapping of polyglycine radical. An aqueous solution of polyglycine (*ca.* 1 m*M*, approximate molecular weight 6000) containing 5 mg/ml MNP was cooled by ice and γ-irradiated at a dose rate of *ca.* 75 Gy/min with a total dose of 0.2 kGy, without deaeration. ESR measurements of the irradiated solution revealed a spin adduct which was assigned the structure

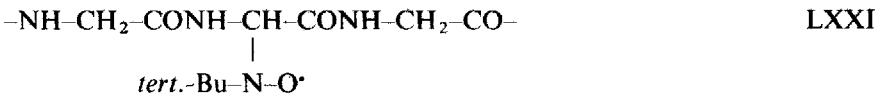

LXXI

the internal backbone adduct from polyglycine. Its h.f.s.c.s at pH 4.7 are a_N = 1.50 mT, $a_{\beta H}$ = 0.25 mT and $a_{\beta N}$ = 0.27 mT. The backbone adduct from polyalanine was reported previously[24].

The spin adducts from dipeptides and tripeptides, whose h.f.s.c.s are summarized in Tables VI and VII, respectively, can be grouped into four general types, as follows: (a) deamino adducts derived from short-lived radicals produced by reductive deaminations upon addition of hydrated electrons to the N-terminal peptide carbonyl groups; (b) C-terminal backbone adducts; (c) internal backbone adducts and (d) side-chain adducts derived from short-lived radicals produced by hydrogen abstractions mainly by hydroxyl radicals, from α-carbon atoms in the C-terminal and internal main chains and a carbon in an aliphatic side-chain, respectively. The detection of the internal backbone adducts from the tripeptides and polypeptides suggest that, in general, short-lived backbone radicals, –CONH–ĊR–CONH–, are produced in γ-irradiated aqueous solutions by hydrogen abstraction from an internal α-carbon atom in the main chains of proteins, mainly by ·OH:

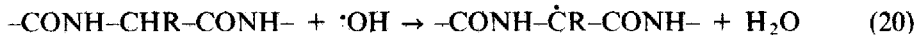

(20)

CONCLUSIONS

The HPLC–ESR method described is expected to be widely applicable for studies on the structures and properties of free radicals, as shown in the present work

by the separation of diastereomeric radicals, the differentiation of their absolute configurations, the determination of pK_a values, the magnetic non-equivalence of the β-H h.f.s.c.s caused by the asymmetry of the δ-carbon atom, etc.

ACKNOWLEDGEMENTS

The authors express their sincere gratitude to Dr. Souji Rokushika, Mr. Nobuhiro Suzuki and Mr. Naohisa Iguchi, Kyoto University, for their invaluable contributions.

REFERENCES

1 W. A. Pryor (Editor), *Free Radicals in Biology*, Vols. 1–5 (1976–1982), Academic Press, New York, and references therein.
2 H. Dertinger and H. Jung, *Molecular Radiation Biology*, Springer, Berlin, 1st ed., 1970, and references therein.
3 T. Henriksen, T. B. Melø and G. Saxebøl, in W. A. Pryor (Editor), *Free Radicals in Biology*, Vol. 2, Academic Press, New York, 1976, Ch. 8, and references therein.
4 E. G. Janzen and B. J. Blackburn, *J. Am. Chem. Soc.*, 90 (1968) 5909.
5 E. G. Janzen, *Acc. Chem. Res.*, 4 (1971) 31, and references therein.
6 C. Lagercrantz and S. Forshult, *Nature (London)*, 218 (1968) 1247.
7 C. Lagercrantz, *J. Phys. Chem.*, 75 (1971) 3466, and references therein.
8 G. R. Chalfont and M. J. Perkins, *J. Am. Chem. Soc.*, 89 (1967) 3054.
9 M. J. Perkins, *Adv. Phys. Org. Chem.*, 17 (1980) 1, and references therein.
10 S. Terabe and R. Konaka, *J. Am. Chem. Soc.*, 91 (1969) 5655.
11 I. H. Leaver and G. C. Ramsey, *Tetrahedron*, 25 (1969) 5669.
12 E. G. Janzen, in W. A. Pryor (Editor), *Free Radicals in Biology*, Vol. 4, Academic Press, New York, 1980, Ch. 4, and references therein.
13 P. B. McCay, T. Noguchi, K.-L. Fong, E. K. Lai and J. L. Poyer, in W. A. Pryor (Editor), *Free Radicals in Biology*, Vol. 4, Academic Press, New York, 1980, Ch. 5, and references therein.
14 C. Lagercrantz, *J. Am. Chem. Soc.*, 95 (1973) 220.
15 H. Taniguchi and H. Hatano, *Chem. Lett.*, (1974) 531.
16 H. Taniguchi and H. Hatano, *Chem. Lett.*, (1975) 9.
17 K. N. Jobin, A. W. Johnson, M. F. Lappert and B. K. Nicholson, *J. Chem. Soc., Chem. Commun.*, (1975) 441.
18 A. Joshi, S. Rustgi and P. Riesz, *Int. J. Radiat. Biol. Relat. Stud. Phys. Chem. Med.*, 30 (1976) 151.
19 S. Rustgi and P. Riesz, *Int. J. Radiat. Biol. Relat. Stud. Phys. Chem. Med.*, 33 (1978) 21.
20 S. Rustgi and P. Riesz, *Radiat. Res.*, 75 (1978) 1.
21 A. Joshi, H. Moss and P. Riesz, *Int. J. Radiat. Biol. Relat. Stud. Phys. Chem. Med.*, 34 (1978) 165.
22 S. Rustgi, A. Joshi, H. Moss and P. Riesz, *Int. J. Radiat. Biol. Relat. Stud. Phys. Chem. Med.*, 31 (1977) 415.
23 S. Rustgi, A. Joshi, P. Riesz and F. Friedberg, *Int. J. Radiat. Biol. Relat. Stud. Phys. Chem. Med.*, 32 (1977) 533.
24 A. Joshi, S. Rustgi, H. Moss and P. Riesz, *Int. J. Radiat. Biol. Relat. Stud. Phys. Chem. Med.*, 33 (1978) 205.
25 S. Rustgi and P. Riesz, *Int. J. Radiat. Biol. Relat. Stud. Phys. Chem. Med.*, 34 (1978) 127.
26 S. Rustgi and P. Riesz, *Int. J. Radiat. Biol. Relat. Stud. Phys. Chem. Med.*, 34 (1978) 449.
27 P. Riesz and S. Rustgi, *Radiat. Phys. Chem.*, 13 (1979) 21.
28 S. Rokushika, H. Taniguchi and H. Hatano, *Anal. Lett.*, 8 (1975) 205.
29 S. Kominami, S. Rokushika and H. Hatano, *Int. J. Radiat. Biol. Relat. Stud. Phys. Chem. Med.*, 30 (1976) 525.
30 S. Kominami, S. Rokushika and H. Hatano, *Radiat. Res.*, 72 (1977) 89.
31 M. H. Klapper and M. Faraggi, *Quart. Rev. Biophys.*, 12 (1979) 465, and references therein.
32 B. H. J. Bielski and J. M. Gebicki, in W. A. Pryor (Editor), *Free Radicals in Biology*, Vol. 3, Academic Press, New York, 1977, Ch. 1, and references therein.

33 J. C. Stowell, *J. Org. Chem.*, 36 (1971) 3055.
34 K. Makino, N. Suzuki, F. Moriya, S. Rokushika and H. Hatano, *Anal. Lett.*, 13 (1980) 311.
35 K. Makino, N. Suzuki, F. Moriya, S. Rokushika and H. Hatano, *Radiat. Res.*, 86 (1981) 294.
36 C. N. R. Rao and K. R. Bhaskar, in H. Feuer (Editor), *The Chemistry of the Nitro and Nitroso Group*, Part 1, Interscience, New York, 1969, Ch. 3, and references therein.
37 K. Makino, N. Suzuki, F. Moriya, S. Rokushika and H. Hatano, *Chem. Lett.*, (1979) 675.
38 K. Makino, *J. Phys. Chem.*, 84 (1980) 1012.
39 U. Deffner and W. Schimmack, *Int. J. Radiat. Biol. Relat. Stud. Phys. Chem. Med.*, 29 (1976) 71.
40 D. F. Bowman, T. Gillan and K. U. Ingold, *J. Am. Chem. Soc.*, 93 (1971) 6555.
41 W. Brackman and C. J. Gaasbeek, *Rec. Trav. Chim. Pays-Bas*, 85 (1966) 221.
42 K. Makino, M. M. Massoba and P. Riesz, *Radiat. Res.*, 95 (1983) 519.
43 F. Moriya, K. Makino, N. Suzuki, S. Rokushika and H. Hatano, *J. Phys. Chem.*, 84 (1980) 3085.
44 W. M. Garrison, *Radiat. Res. Rev.*, 3 (1972) 305, and references therein.
45 M. D. Sevilla, *J. Phys. Chem.*, 74 (1970) 2096.
46 H. Taniguchi, K. Fukui, S. Ohnishi, H. Hatano, H. Hasegawa and T. Maruyama, *J. Phys. Chem.*, 72 (1968) 1926.
47 P. Neta, M. Simic and E. Hayon, *J. Am. Chem. Soc.*, 74 (1970) 4763.
48 P. Neta, M. Simic and E. Hayon, *J. Phys. Chem.*, 75 (1971) 738.
49 Y. Kirino, *J. Phys. Chem.*, 79 (1975) 1296.
50 B. C. Gilbert and M. Trenwith, *J. Chem. Soc., Perkin Trans. 2*, (1973) 1834.
51 K. Makino, N. Suzuki, F. Moriya, S. Rokushika and H. Hatano, *Anal. Lett.*, 13 (1980) 301.
52 K. Makino, *J. Phys. Chem.*, 84 (1980) 1016.
53 K. Makino, *J. Phys. Chem.*, 84 (1980) 1968.
54 K. Makino and H. Hatano, *Chem. Lett.*, (1979) 119.
55 K. Makino, *J. Phys. Chem.*, 83 (1979) 2520.
56 N. Iguchi, F. Moriya, K. Makino, S. Rokushika and H. Hatano, *Can. J. Chem.*, 62 (1984) 1722.
57 N. Suzuki, K. Makino, F. Moriya, S. Rokushika and H. Hatano, *J. Phys. Chem.*, 85 (1981) 263.
58 F. Moriya, K. Makino, N. Iguchi, N. Suzuki, S. Rokushika and H. Hatano, *J. Phys. Chem.*, 88 (1984) 2373.
59 A. L. J. Beckwith and R. O. C. Norman, *J. Chem. Soc. B*, (1969) 400, and references therein.
60 L. Jonkman, H. Muller and J. Kommandeur, *J. Am. Chem. Soc.*, 93 (1971) 5833.
61 F. W. King, *Chem. Rev.*, 76 (1976) 157, and references therein.
62 F. Moriya, K. Makino, N. Suzuki, S. Rokushika and H. Hatano, *J. Phys. Chem.*, 84 (1980) 3614.
63 F. Moriya, K. Makino, N. Suzuki, S. Rokushika and H. Hatano, *J. Am. Chem. Soc.*, 104 (1982) 830.
64 F. Moriya, N. Iguchi, K. Makino, S. Rokushika and H. Hatano, *Can. J. Chem.*, 62 (1984) 2206.